Appl Phys B (2010) 98: 311–315
DOI 10.1007/s00340-009-3747-x

Applied Physics B
Lasers and Optics

Q-switched operation of an in-band-pumped Ho:LuAG laser with kilohertz pulse repetition frequency

B.-Q. Yao · X.-M. Duan · L. Ke · Y.-L. Ju · Y.-Z. Wang · G.-J. Zhao

Received: 9 June 2009 / Revised version: 4 August 2009 / Published online: 20 November 2009

Abstract We report continuous-wave (CW) and repetitively Q-switched operation of an in-band-pumped Ho:LuAG laser at room temperature. End-pumped by a Tm:YLF solid-state laser with emission wavelength of 1.91 μm, the CW Ho:LuAG laser generated 5.4-W output at 2100.7 nm with beam quality factor of $M^2 \sim 1.03$ for an incident pump power of 14.1 W, corresponding to slope efficiency of 67% with respect to absorbed pump power. Up to 1.5-mJ energy per pulse at pulse repetition frequency (PRF) of 3 kHz and 4.5-W average power with FWHM pulse width of 28 ns at 5 kHz were demonstrated in repetitively Q-switched operation.

PACS 42.55.Rz · 42.60.Pk · 42.60.Gd

1 Introduction

2-μm repetitively Q-switched lasers have a variety of applications for range finding, long-range environmental sensing, and Doppler radar wind detecting [1]. It can be used to drive nonlinear optical parametric oscillator (OPO) based on materials such as $ZnGeP_2$ or orientation-patterned GaAs to efficiently produce coherent radiation in the 3–12 μm spectral region [2, 3]. The large emission cross section of the Ho^{3+} system (compared to Tm^{3+} system) make it preferable for generation of nanosecond-class pulses with high peak power. The direct resonant pumping Ho $^5I_7$ manifold offers the advantages of high slope efficiency and minimal heating owing to inherent low quantum defect of less than 10% between pump and laser. Resonantly pumped Ho lasers based on YAG and YLF host materials have been extensively investigated for generation of high power and high pulse energy 2-μm laser by Budni et al. [4], Lippert et al. [5], and Dergachev et al. [6]. Due to its excellent mechanical properties similar to those of YAG, lutetium aluminum garnet ($Lu_3Al_5O_{12}$, LuAG) has been received significant attention as attractive host for laser ions, such as Er^{3+} at 1.66 μm and Yb^{3+} at 1.0 μm [7, 8]. LuAG has significant advantages that make it well suited for Ho^{3+} ions doping to produce efficiently 2-μm radiation at room temperature. Ho:LuAG has a higher crystal field than Ho:YAG resulting in a large manifold splitting and a low thermal occupation for the lower laser level. Compared to 9 other garnet laser materials considered, Ho:LuAG has the highest branching ratio for a level in the $^5I_7$ manifold at room temperature [9]. And the slight molar mass difference of 5.8% between Ho and Lu (46.7% between Y and Ho) makes a weak decrease in thermal conductivity of LuAG with holmium doping [10].

As to Ho^{3+}-doped lutetium aluminum garnet, Scholle et al. achieved CW 18 mW of single-mode laser output from a diode-pumped Ho:Tm:LuAG laser [11], Hart et al. demonstrated 10 mJ of output energy from a free-running Ho:LuAG laser end-pumped by a pulsed $Co:MgF_2$ laser at 1878 nm [12], and Barnes et al. reported on a pulsed Ho:Tm:LuAG laser in normal mode with output energy up to 2.6 mJ by using a $Ti:Al_2O_3$ as the pump source [13]. However, repetitively Q-switched laser with pulse repetition frequency (PRF) up to several kilohertz has not been performed in resonantly pumped Ho:LuAG laser. Here we re-

B.-Q. Yao (✉) · X.-M. Duan · L. Ke · Y.-L. Ju · Y.-Z. Wang
National Key Laboratory of Tunable Laser Technology, Harbin Institute of Technology, Harbin 150001, China
e-mail: yaobq08@hit.edu.cn
Fax: +86-451-86412720

G.-J. Zhao
Key Laboratory of Material Science and Technology for High Power Lasers, Shanghai Institute of Optics and Fine Mechanics, Chinese Academy of Sciences, Shanghai 201800, China

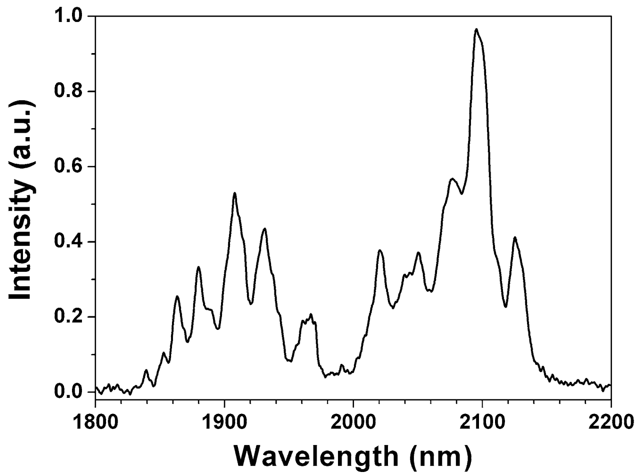

Fig. 1 Room-temperature Ho:LuAG $^5I_7 \rightarrow {}^5I_8$ fluorescence spectrum

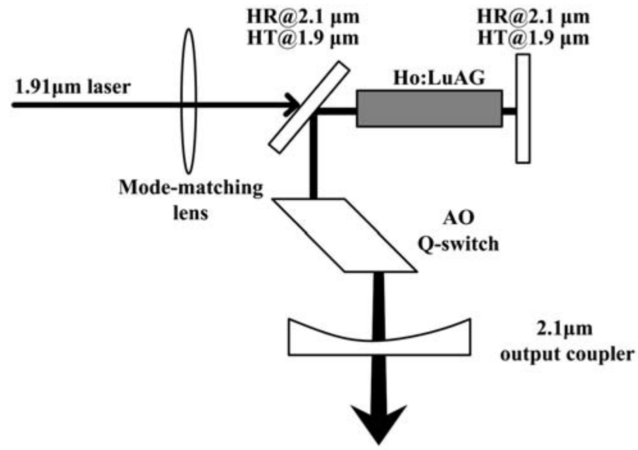

Fig. 2 Schematic diagram of a Ho:LuAG laser pumped by a 1.91 µm Tm:YLF laser

port efficient Q-switched emission from a Ho:LuAG laser pumped in-band at 1.91 µm.

2 Emission spectrum

The laser crystals used here were grown by a standard Czochralski technique. The Ho:LuAG crystal has a Ho^{3+} level of 0.8 at.%, corresponding to a density of 1.13×10^{20} ions/cm^3. Ho:LuAG has similar absorption and emission parameters to Ho:YAG. According to the spectral feature from [12], the absorption peaks near 1.9 µm are located at 1.88 and 1.91 µm with corresponding absorption cross section of approximately 0.76×10^{-20} cm^2, which coincide with Tm:YLF laser emission wavelengths. As LuAG is a cubic material, only one emission spectrum was measured. Figure 1 shows the fluorescence spectrum from Ho^{3+} $^5I_7 \rightarrow {}^5I_8$ transitions in Ho:LuAG, which was excited by a 1.91 µm Tm:YLF laser. A 300 mm WDM1-3 monochromator with a 600 lines/mm grating blazed for 2.0 µm was used to scan across the spectrum (0.8-nm resolution). The fluorescence was monitored by an InGaAs detector with a SRS830 lock-in amplifier for signal extraction. The spectrum has not been corrected for grating and detector response. As shown in Fig. 1, the spectra for Ho:LuAG is similar to that for Ho:YAG, but the emission of Ho:LuAG is shifted about 4 nm to longer wavelength. The subtle changes of energy levels resulting from replacing Y with Lu in Ho:YAG results in slightly different transition wavelengths than in Ho:LuAG. The lifetime of Ho $^5I_7$ manifold for LuAG was measured to be 7.6 ms by using a 2.05-µm Q-switched Tm, Ho:GdVO$_4$ laser (10 Hz PRF, 20-ns pulse duration) as an exciting source, comparing with 8 ms for Ho:YAG [9].

3 Laser arrangement

The schematic diagram of Ho:LuAG laser is shown in Fig. 2. To evaluate the lasing performance of Ho:LuAG crystal in room temperature, a diode-pumped Tm:YLF laser with emission wavelength of 1.91 µm was utilized for pumping, which emits 15 W of output power with beam quality M^2 of ∼1.1. The absorption coefficient of Ho:LuAG is about 0.86 cm^{-1} at 1.91 µm.

The calculated up-conversion parameter with a quantum mechanical model in Ho:LuAG is 16.8×10^{-18} cm^3/s, compared with 11.9×10^{-18} cm^3/s in Ho:YAG [14]. Note that the up-conversion rate from the upper laser level in Ho:LuAG depends on the holmium doping concentration, and the up-conversion losses become less significant with the lower concentration of less than 1% [15]. So a Ho^{3+}-doping concentration of 0.8 at.% was chosen in our experiment. The Ho:LuAG crystal is 5 mm in diameter and 25 mm in length. The optimal product (2% cm) of the crystal length and the doping concentration is in principle determined by a trade-off between the pump absorption efficiency and the increase in laser threshold resulting from the quasi-three-level nature. At low pump power, the single-pass absorption of the crystal was measured to be 82%. The laser crystal was wrapped in indium foil and clamped in a copper heat sink held at a temperature of 15°C with a thermoelectric cooler. The Ho laser resonator, also shown in Fig. 2, consists of a plane mirror with $R > 99.5\%$ at 2.1 µm, a 45° dichroic mirror with $R > 99.5\%$ at 2.1 µm, and $T > 98\%$ at 1.91 µm, and an output coupler with curvature radius of 100 mm. The physical cavity length is about 67 mm resulting in an estimated resonant mode size of ∼360 µm in the crystal with an analysis of cold resonator. By the use of a 200 mm focal length mode-matching lens, pump spot size of ∼360 µm in diameter was formed in the Ho crystal. A 30-mm-long Brewster-cut acousto-optic Q-switch (Gooch

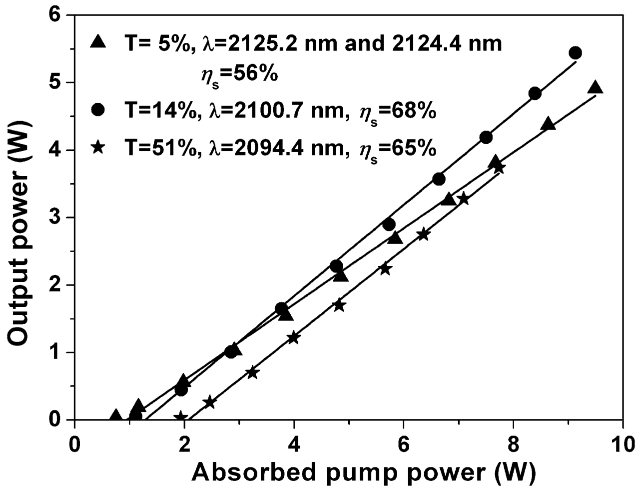

Fig. 3 Output performance of CW Ho:LuAG laser

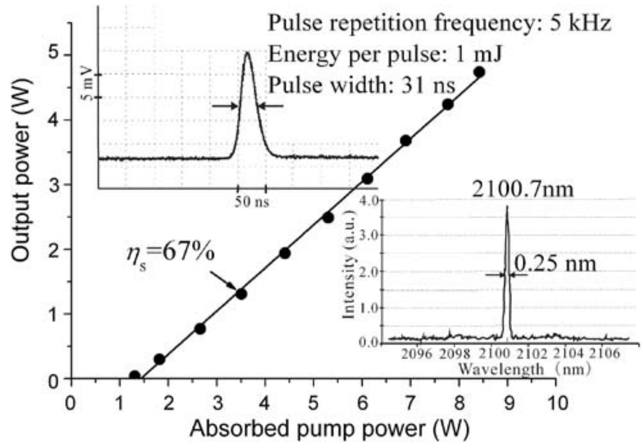

Fig. 4 Output power of Ho:LuAG laser at 5 kHz PRF versus absorbed pump power. *Inset*: typical temporal pulse shape (*upper*) and the spectral output of the Ho:LuAG laser (*lower*)

& Housego Ltd.) with an acoustic aperture of 1.8 mm is the central component for repetitively Q-switched operation. The acousto-optic modulator (AOM) material is crystal quartz with 99.6% transmission for 2.1 µm operation. It is rated for 20-W radio-frequency (RF) input power at frequency of 40.7 MHz. The modulation loss (with vertical polarization) is greater than 45%, which is adequate to hold off the intracavity laser actions.

4 Laser results

The CW operation of Ho:LuAG laser was performed ahead of the AO Q-switched laser experiments. We investigated the output characteristics of the laser for different output couplers with transmissions of 5, 14, and 51%, respectively. Figure 3 shows the measured output power of the Ho:LuAG laser versus the absorbed pump power. The highest efficiency operation was achieved by a transmission coupler of $T = 14\%$. The maximum output power was 5.4 W for an absorbed pump power of 9.1 W. The slope efficiency of 68% was achieved with respect to absorbed pump power. With $T = 5$ and 51%, the slope efficiencies responding to absorbed pump power were 56 and 65%, respectively. The spectral output of the Ho:LuAG laser was measured with a Burleigh WA-650 spectrum analyzer combined with a WA-1500 wavemeter. For $T = 5\%$, the emission oscillates at 2124.4 and 2125.2 nm. For $T = 14\%$, the emission line was centered on 2100.7 nm with a FWHM linewidth of 0.25 nm. For $T = 51\%$, the emission line was located at 2094.4 nm.

In Q-switched experiment, we chose 2100.7-nm transition as operating wavelength, which exhibited better CW performance than the other two transitions of 2094.4 and 2125.2 nm. The output coupler of $T = 29\%$ was employed for reducing intracavity energy fluence. The PRF was greater than or equal to 3 kHz to keep the fluerence in

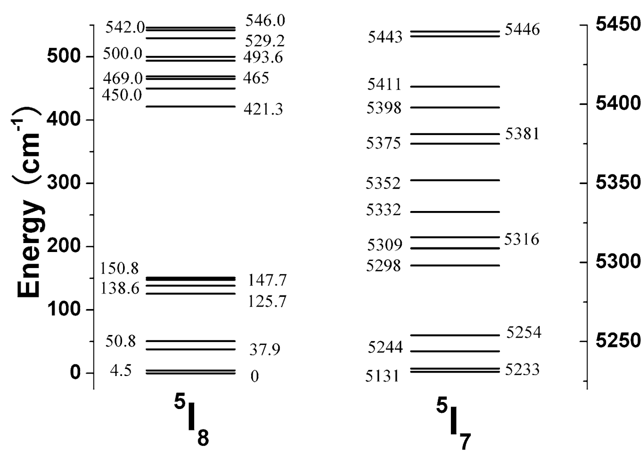

Fig. 5 Energy level diagram of Ho^{3+} in LuAG at 8 K

the laser cavity well below the damage threshold. Typical temporal pulse shape for PRF of 5 kHz is shown in Fig. 4 inset, which is reasonably symmetrical with a 31 ns FWHM pulse width at output energy per pulse of 0.95 mJ. As listed in Table 1, the pulse duration increase from 24 ns at 3 kHz to 31 ns at 5 kHz. Repetitively Q-switched operation at 3 kHz yielded the maximum output energy per pulse of 1.5 mJ with a peak power of 62.5 kW. The Q-switch RF off-time was set to be 4.2 µs, which is long enough to allow laser pulses to build up in the resonator. The pulse buildup time was measured to be 0.76, 0.74, and 0.72 µs at PRF of 5, 4, and 3 kHz, respectively. The pulse-to-pulse jitter was serious when the output energy per pulse was less than 0.3 mJ but it became relatively stable when greater than 0.5 mJ per pulse was attained. The pulse amplitude stability was measured at approximately ±12.5% about the mean at average output power of 4.75 W and PRF of 5 kHz.

According to Stark-split ground and first excited states in Ho^{3+}:LuAG at 8 K [16] (see Fig. 5), 2100 nm laser trans-

Table 1 Performance of Q-switched Ho:LuAG laser

PRF (kHz)	Energy per pulse (mJ)	Pulse width (ns)	Peak power (kW)	Pulse build-time (µs)
3	1.50	24	62.5	0.72
4	1.17	28	41.8	0.74
5	0.95	31	30.6	0.76

Table 2 Population fraction of Ho^{3+} $^5I_7$ and $^5I_8$ in the laser and pump levels for LuAG and YAG at 300 K

	f_l	f_u	f_a	f_b	f_T	f_x
LuAG	0.0147	0.1036	0.140	0.0978	0.125	1.700
YAG	0.0172	0.0998	0.154	0.0998	0.147	1.647

fers from the 5231 cm^{-1} level of $^5I_7$ manifold to 469 cm^{-1} level of the ground-state $^5I_8$ manifold. Table 2 shows a summary of the population fraction of $^5I_7$ and $^5I_8$ ions in the pump and laser levels for Ho:LuAG and Ho:YAG at 300 K where f_l and f_u are the population fraction of $^5I_7$ and $^5I_8$ manifolds in the lower and upper laser Stark levels, f_a and f_b are the population fraction of the lower and the upper Stark levels of the pump transition, $f_T = f_l/(f_l + f_u)$ is the fraction of ions needed to be excited to the upper laser level to obtain optical transparency on the laser transition, and $f_x = (1 + f_b/f_a)$ is related to pump absorption efficiency, which accounts for both ground-state depletion (the "1") and population buildup in the upper manifold (f_b/f_a). A larger value of f_x means a lower absorption efficiency for the pump transition [15]. As seen from Table 1, the terminal level of $^5I_8$ manifold is only ∼1.47%-populated at 300 K for Ho:LuAG (1.72% for Ho:YAG), which means that the laser is a nearly four-level system [17]. We estimate that only ∼12.5% of the Ho^{3+} ions need to be excited for achievement of transparency at the emission wavelength in LuAG, compared to ∼14.7% in YAG. The slight reduced lower laser thermal population for Ho:LuAG lasers will improve performance of $^5I_7 \rightarrow {}^5I_8$ lasing at ∼2.1 µm compared to Ho:YAG lasers.

Figure 6 inset shows the evolution of the Ho:LuAG laser beam propagation at the 5.4-W output power level in CW mode after it has been passed through a positive 200-mm focal length lens. We estimated the beam quality to be $M^2 = 1.03 \pm 0.02$ clearly indicating nearly diffraction-limited beam propagation.

5 Conclusion

In conclusion, CW and Q-switched operation of a resonantly pumped Ho:LuAG laser emitting at around 2.1 µm is demonstrated, generating up to 5.3 W of CW output power with near-diffraction-limited beam quality of $M^2 \sim 1.03$, and up to 1.5 mJ of energy per pulse with peak power as high as 62.5 kW at PRF of 3–5 kHz.

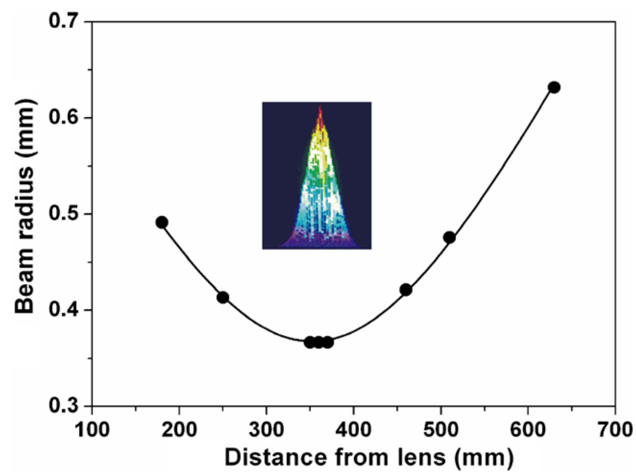

Fig. 6 M^2 measurement of the Ho:LuAG laser output at the 5.4-W output power level. *Inset*: typical 3D beam profiles taken by a Spiricon Pyrocam I pyroelectric camera

Acknowledgements This work was supported by National Natural Science Foundation of China under Grant No. 60878011 and also supported by Acknowledge Innovation Program of Chinese Academy of Sciences.

References

1. T.J. Carrig, Proc. SPIE **5620**, 187 (2004)
2. P.A. Budni, L.A. Pomeranz, M.L. Lemons, C.A. Miller, J.R. Mosto, E.P. Chicklis, J. Opt. Soc. Am. B **17**, 723 (2000)
3. C. Kieleck, M. Eichhorn, A. Hirth, D. Faye, E. Lallier, Opt. Lett. **34**, 262 (2009)
4. P.A. Budni, M.L. Lemons, J.R. Mosto, E.P. Chicklis, IEEE J. Sel. Top. Quantum Electron. **6**, 629 (2000)
5. E. Lippert, S. Nicolas, G. Arisholm, K. Stenersen, A.S. Villanger, G. Rustad, Proc. SPIE **6397**, 639704 (2006)
6. A. Dergachev, D. Armstrong, A. Smith, T. Drake, M. Dubois, Opt. Express **15**, 14404 (2007)
7. S.D. Setzler, K.J. Snell, T.M. Pollak, P.A. Budni, Y.E. Young, E.P. Chicklis, Opt. Lett. **28**, 1787 (2003)
8. J. Dong, K. Ueda, A.A. Kaminskii, Opt. Lett. **32**, 3266 (2007)
9. E.D. Filter, N.P. Barnes, F.L. Naranjo, L. Felipe, M.R. Kokta, in *Advanced Solid State Lasers (ASSL)* (1993), paper: ML5

10. R. Gaumé, B. Viana, D. Vivien, J.P. Roger, D. Fournier, Appl. Phys. Lett. **83**, 1355 (2003)
11. K. Scholle, E. Heumann, G. Huber, Laser Phys. Lett. **1**, 285 (2004)
12. D.W. Hart, M. Jani, N.P. Barnes, Opt. Lett. **21**, 728 (1996)
13. N.P. Barnes, E.D. Filer, F.L. Naranjo, W.J. Rodriguez, M.R. Kokta, Opt. Lett. **18**, 708 (1993)
14. N.P. Barnes, B.M. Walsh, E.D. Filter, J. Opt. Soc. Am. B **20**, 1212 (2003)
15. E. Lippert, S. Nicolas, G. Arisholm, K. Stenersen, G. Rustad, Appl. Opt. **45**, 3839 (2006)
16. M. Walsh, G.W. Grew, N.P. Barnes, J. Phys. Chem. Solids **67**, 1567 (2006)
17. S.D. Setzler, M.P. Francis, Y.E. Young, J.R. Konves, E.P. Chicklis, IEEE J. Quantum Electron. **11**, 645 (2005)